International Conference on
Environmentally Sound Water Resources Utilization
Bangkok, Thailand, 8-11 November 1993

FLOOD FLOW ANALYSIS IN URBAN AREAS

Atsuyoshi MIURA
Yasuyuki SHIMIZU

Civil Engineering Research Institute, 062 Hiragishi 1-3
Toyohiraku Sapporo, Japan

ABSTRACT

Flood frequencies in urban areas have recently been very low due to the development of flood control systems. However, a single flood may cause severe damage to urban areas due to the concentration of population and property. City planning for streets, buildings, parks, roadside trees, and refuge areas does not always consider flood flows. As a result flood flows may converge on certain refuges. There is a pressing need for a model to accurately predict the behavior of flood flows in urban areas with complicated layouts of streets and buildings.

INTRODUCTION

Assuming that floods occur in the Toyohira River which runs through Sapporo City, this study uses a two-dimensional model to consider the relation between the layout of streets and buildings and the damage caused by flood flows. The characteristics of flood flows were also studied.

BASIC EQUATION

Flood flow may be regarded as a two-dimensional plane flow and the basic equations which describe this kind of fluid motion are as follows:

the continuity equation

$$\frac{\partial h}{\partial t} + \frac{\partial M}{\partial x} + \frac{\partial N}{\partial y} = 0 \tag{1}$$

the momentum equation in the x-direction

$$\frac{\partial M}{\partial t} + \frac{\partial (uM)}{\partial x} + \frac{\partial (vM)}{\partial y} = -gh\frac{\partial H}{\partial x} - \frac{\tau_x}{\rho} + \frac{\partial}{\partial x}\left(\varepsilon\frac{\partial M}{\partial x}\right) + \frac{\partial}{\partial y}\left(\varepsilon\frac{\partial M}{\partial y}\right) \tag{2}$$

the momentum equation in the y-direction

$$\frac{\partial N}{\partial t} + \frac{\partial (uN)}{\partial x} + \frac{\partial (vN)}{\partial y} = -gh\frac{\partial H}{\partial y} - \frac{\tau_y}{\rho} + \frac{\partial}{\partial x}\left(\varepsilon\frac{\partial N}{\partial x}\right) + \frac{\partial}{\partial y}\left(\varepsilon\frac{\partial N}{\partial y}\right) \tag{3}$$

where, x, y = are Cartesian coordinates; u, v = flow velocities in the x-, y-directions: h = depth; H = elevation of the water surface; ρ = density of flowing fluid; ε = eddy viscosity coefficient: g = gravity;τ_x, τ_y = bottom shear stresses in the x-, y-directions; t = time: M, N = discharge fluxes (discharge per unit width) in the x-, y-directions; and $M = uh, N = vh$.

NUMERICAL CALCULATION METHOD

Differential calculus is used for the actual numerical calculation of the continuity eqvation and momentum equations, in the x-, and y-directions.
The lattice and calculation points in Figure-1 are arranged according to Shimizu[1], and,dx, dy, $\Delta\ x$, and $\Delta\ y$ are defined to fit the calculation as shown in Figure-2.

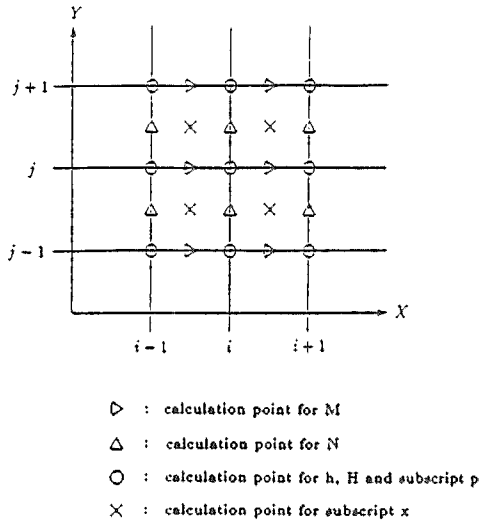

Figure-1 Calculation lattice and calculation points

Finite differences of the continuity equation,

$$h(i,j,t+\Delta t) = -(A1 + A2)\Delta t + h(i,j,t) \qquad (4)$$

where

$$A1 = \frac{M(i+1,j) - M(i,j)}{\Delta x} \qquad (5)$$

$$A2 = \frac{N(i,j+1) - N(i,j)}{\Delta y} \qquad (6)$$

Finite differences in the x-direction of the momentum equation,

$$M_t(i,j) = -\frac{B_1 + B_2 + B_3 + B_4 + B_5 - B_6 - B_7}{A_1 + A_5} \qquad (7)$$

here M_t indicates the value of M after $\Delta\ t$ hours have passed. The A and B terms are the total of the differential terms of equation (2) and the numbers show the order from the left of the equation (2). The differences in each term of equation (2) are as follows:
The difference in the first term is

$$\frac{\partial M}{\partial t} = A_1 + B_1 \qquad (8)$$

where

$$A_1 = \frac{1}{\Delta t} M_t(i,j) \qquad (9)$$

$$B_1 = -\frac{1}{\Delta t} M(i,j) \qquad (10)$$

The difference in the second term is

$$\frac{\partial}{\partial x}\left(\frac{M^2}{h}\right) = B_2 \qquad (11)$$

where

$$B_2 = \left\{ \frac{M_p(i,j)^2}{h(i,j)} - \frac{M_p(i-1,j)^2}{h(i-1,j)} \right\} \Big/ dx \qquad (12)$$

where, $u = M/h$ and M_p is the value of M at the calculation point p in Figure-1.
The difference in third term is

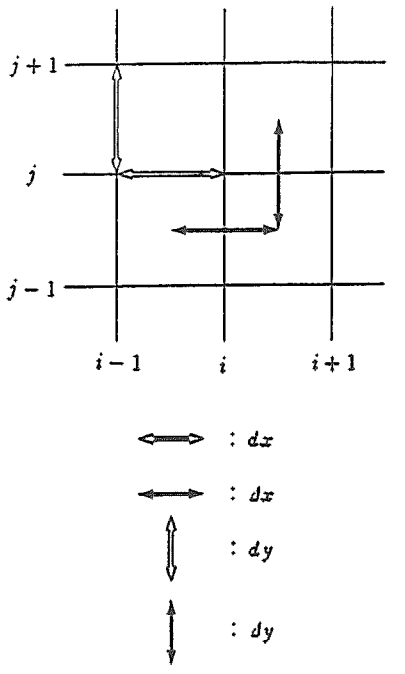

Figure-2 Definition of dx,dy, Δ x, Δ y

$$\frac{\partial}{\partial y}\left(\frac{NM}{h}\right) = B_3 \tag{13}$$

where

$$B_3 = \left\{\frac{N_x(i,j+1)M_x(i,j+1)}{h_x(i,j+1)} - \frac{N_x(i,j)M_x(i,j)}{h_x(i,j)}\right\} \Big/ \Delta y \tag{14}$$

and $v = N/h$. The M_x, N_x, h_x , terms are the values at x in Figure-1, at the calculation point. The difference in the fourth term is

$$gh\frac{\partial H}{\partial x} = B_4 \tag{15}$$

where

$$B_4 = g\frac{h(i,j)+h(i-1,j)}{2}\frac{H(i,j)-H(i-1,j)}{dx} \tag{16}$$

The difference in the fifth term is

$$\frac{\tau_x}{\rho} = -A_5 M_t(i,j) - B_5 \tag{17}$$

where

$$A_5 = \frac{gn^2}{2}\sqrt{M(i,j)^2 + Nu(i,j)^2} \Big/ \left\{\frac{h(i,j)-h(i-1,j)}{2}\right\}^{\frac{7}{3}} \tag{18}$$

$$B_5 = -A_5 M(i,j) \tag{19}$$

Aiso, in A_5 , n = Manning's coefficient of roughness, and

$$n = \frac{n_p(i-1,j)+n_p(i,j)}{2} \tag{20}$$

where n_p is the value of n at p in Figure-1, and

$$N_u = \frac{N(i,j)+N(i,j+1)+N(i-1,j)+N(i-1,j-1)}{4} \tag{21}$$

However,

$$\frac{\tau_x}{\rho} = \frac{gn^2 u\sqrt{u^2+v^2}}{h^{\frac{1}{3}}} \tag{22}$$

is applied.
The difference in the sixth terms is

$$\frac{\partial}{\partial x}\left(\varepsilon\frac{\partial M}{\partial x}\right) = B_6 \tag{23}$$

where

$$B_6 = \frac{1}{dx^2}\left[\varepsilon_p(i,j)\{M(i+1,j)-M(i,j)\} - \varepsilon_p(i-1,j)\{M(i,j)-M(i-1,j)\}\right] \tag{24}$$

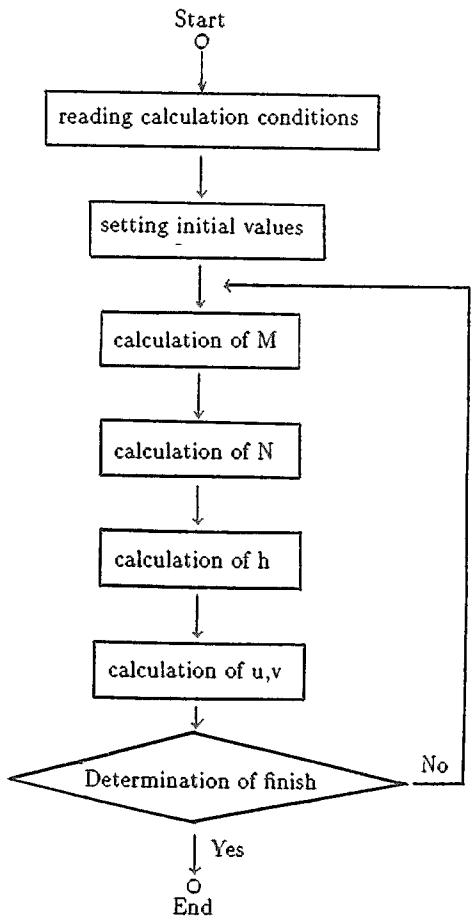

Figure-3 Calculation flow chart

However,

$$\varepsilon_p(i,j) = \frac{\kappa}{6}\sqrt{\tau_p}h(i,j) \tag{25}$$

Where, ε_p is the value of ε at p in Figure-1, and
κ = Karman's constant (κ =0.4)

$$\tau_p = (gn_p(i,j)^2(u(i,j)^2 + v(i,j)^2))/h(i,j)^{\frac{1}{3}} \tag{26}$$

where

$$u(i,j) = M_p(i,j)/h(i,j) \tag{27}$$

$$v(i,j) = N_p(i,j)/h(i,j) \tag{28}$$

Further, $\varepsilon_p(i-1,j)$ is obtained in the same manner.
The difference in the seventh terms is

$$\frac{\partial}{\partial y}\left(\varepsilon\frac{\partial M}{\partial y}\right) = B_7 \tag{29}$$

where

$$B_7 = \frac{1}{\Delta y^2}\left[\varepsilon_x(i,j+1)\{M(i,j+1) - M(i,j)\} - \varepsilon_x(i,j)\{M(i,j) - M(i,j-1)\}\right] \tag{30}$$

However,

$$\varepsilon_x(i,j) = \frac{\kappa}{6}\sqrt{\tau_x}h_x(i,j) \tag{31}$$

where, ε_x is the value of ε at x in Figure-1, and

$$\tau_x = (gn_x(i,j)^2(u_x(i,j)^2 + v_x(i,j)^2))/h_x(i,j)^{\frac{1}{3}} \tag{32}$$

And

$$u_x(i,j) = M_x(i,j)/h_x(i,j) \tag{33}$$

$$v_x(i,j) = N_x(i,j)/h_x(i,j) \tag{34}$$

$\varepsilon_x(i,j+1)$ is obtained in the same manner. Differential calculus is also applied to the momentum equation in the y-direction. The above calculation procedure is shown in Figure-3.

BOUNDARY CONDITIONS AT THE LIP OF FLOOD FLOWS

The boundary condition at the lip of a spreading flood is determined by two adjacent water depth calculation lattice points. Here, the spreading in the x-direction is discussed, using the water depth $h(i-1,j), h(i,j)$ as the basis for the discussion.

The boundary conditions at the lip of the flood with a standard depth of 0.001m, are classified into: (1) the depth of both points lower than the standard depth; (2) only one point reaches or exceeds the standard depth; and (3) the depth of both points reach or exceed the standard depth. Here, the necessary condition for the lip of the flow to spread is (2) which will be discussed next.

To determine condition (2), as shown in Figure-4, with a water surface elevation $H(i-1,j), H(i,j)$ is added, and the substituted depth of 0.02m is used. When $h(i,j)$ is lower than the standard depth and the elevation of the water surface is $H(i,j) < H(i-1,j)$, the depth used is $h(i,j) = 0.02m$. This depth is $0m$ after calculating the discharge flux M_t . When the elevation of the water surface $H(i,j) = H(i-1,j)$ and $H(i,j) > H(i-1,j)$, the discharge flux, $M_t = 0m^2/s$.

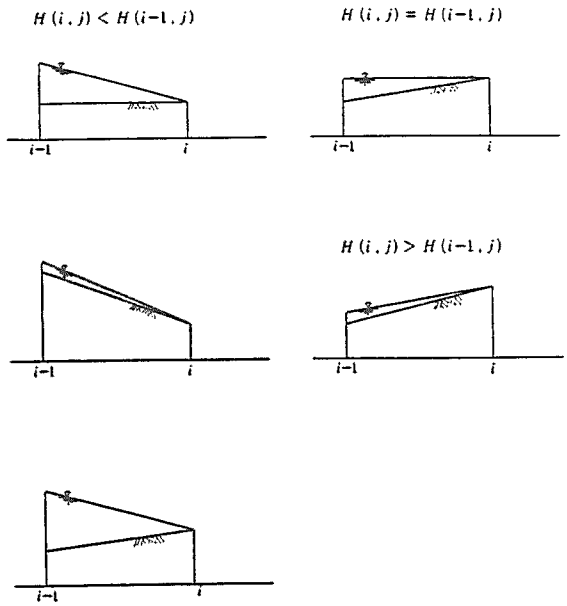

Next, when $h(i-1,j)$ is lower than the standard depth and the elevation of the water surface is $H(i-1,j) < H(i,j)$, after $h(i-1,j) = 0.02m$ has been added, calculations proceed as above. When $H(i-1,j) = H(i,j)$ and $H(i-1,j) > H(i,j)$, the discharge flux,$M_t = 0m^2/s$.

In the y-direction $h(i,j-1), h(i,j)$ is the base for the calculation, similar to the x-direction case.

Figure-4 Concept of flood flow head

CALCULATED RESULTS AND CONDITIONS

A numerical flood flow simulation was conducted for Sapporo city and the Toyohira River.

The left bank of the Toyohira River near the Toyohira Bridge was assumed to be the point where the embankment is breached, because the river channel here is narrow and is also the major bed. If the embankment is breached at this point, damage to the urban area is presumed to be great. The assumed breach is shown in Figure-5, with an assumed length of breach of 150m. The distribution of structures, etc. in this area was taken from Fukuoka et al[2]. The density of structures, etc. was shown as the coefficient of roughness, obtained with a 1:25,000 map. Figure-5 indicates the distribution of the coefficient of roughness and Table-1 shows the coefficient of roughness corresponding to different structure densities. In Figure-5, the hearing colored area shows streets and where the color is lighter the density is greater.

Table-1
Density of structures and coefficient of roughness

density of structures	coefficient of roughness
vacant areas	0.02
streets	0.01
building density 20%	0.03
building density 50%	0.05
building density 80%	0.10
building density over 80%	0.80
rivers, ponds	0.01

One condition specified as a boundary condition was that water will not flow beyond the left bank area of the Toyohira River and not into the hilly area west to Mt. Maruyama. The topography was defined as flat.

The condition for flood waters to flow into the predicted flood-prone area was that the discharge exceeded the design flood discharge to become flood flow. At Kariki on the Toyohira River, the design flood discharge is $2000m^3/s$. Currently, despite improvements and construction of dams upstream of the Toyohira River, flood flows of $2300m^3/s$ can still be anticipated. Therefore,

$300m^3/s$, the volume exceeding the design flood discharge, was assumed to flow into the urban area. Figure-6 is the hydrograph. For the calculations, the flood discharge was set to last 200 minutes. The flood flow discharge was described by using the discharge flux M, N at the assumed breach in the embankment.

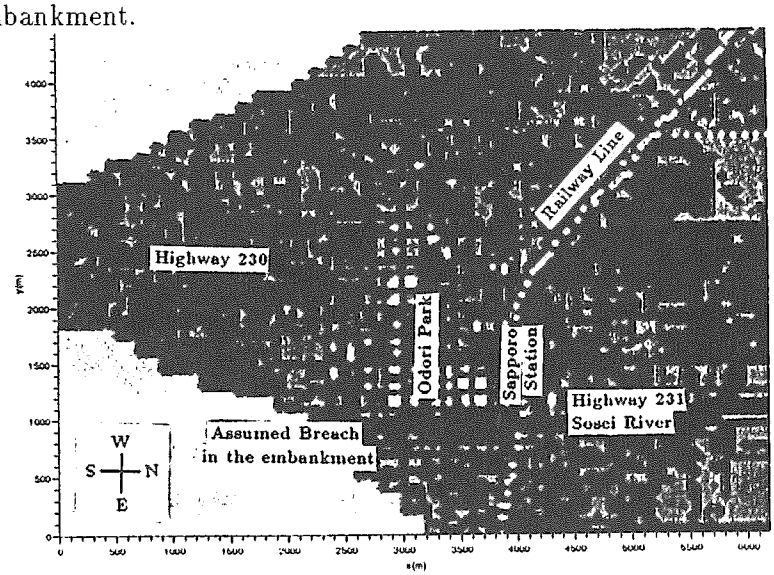

Figure-5 Roughness coefficients

The results of the numerical simulation is shown in Figure-7. The figure shows the situation 200 minutes after flooding started when the flood flow has stopped. The simulation indicates that flood waters flowed along the street network. The depth, flow velocity, and direction at major points in Figure-7 are:$0.24m, 0.22m/s$, to the west at Odori West 8; $0.24m0.17m/s$, to the west at Sapporo Station; $0.25m, 0.14m/s$, to the west at the Clock tower; and $0.14m, 0.38m/s$, to the north at North 14 on Highway 231.

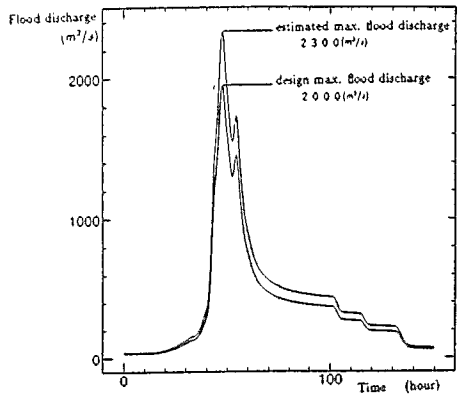

Figure-6 Hydrograph

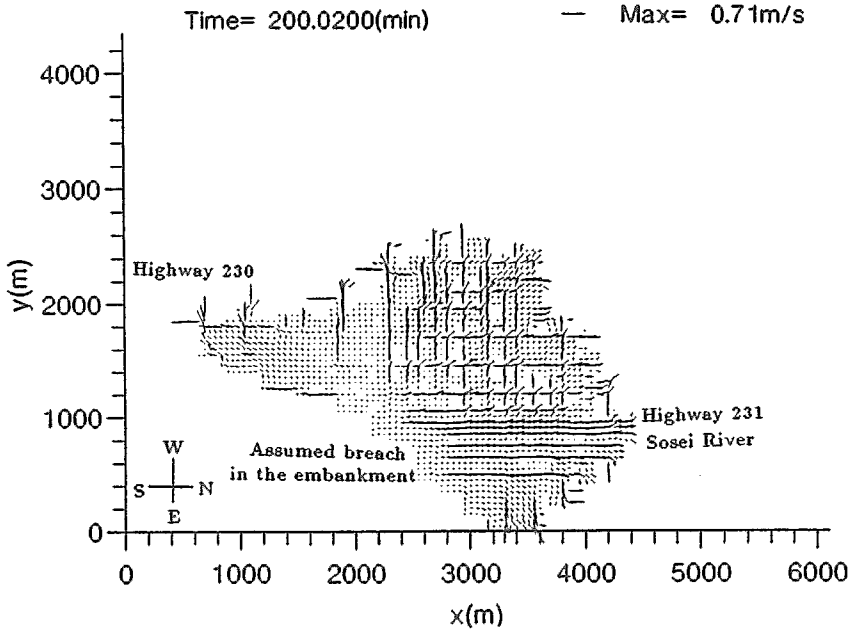

Figure-7 Vector map

ISSUES RELATED TO TOPOGRAPHIC DATA

Along with the calculation of flood flows in the flood flow model, topographic data used in the calculation was examined. Here, national digital information (KS-124-1) has been used for the topographic data. This topographic information[3)] is available as grid data stored on magnetic tape. The national digital information is in the form of maps which digitally describe the whole country. It is in 4,430 sections, each covering an area equivalent to a topographical 1/25,000 map. If this kind of grid data is available for the flood flow calculations, it is possible to adapt such topographic data speedily. Figure-8 is an example of a contour map based on the national digital information (KS-124-1). (To simplify, the area with ground levels above 100m is shown as ground level of 100m.)

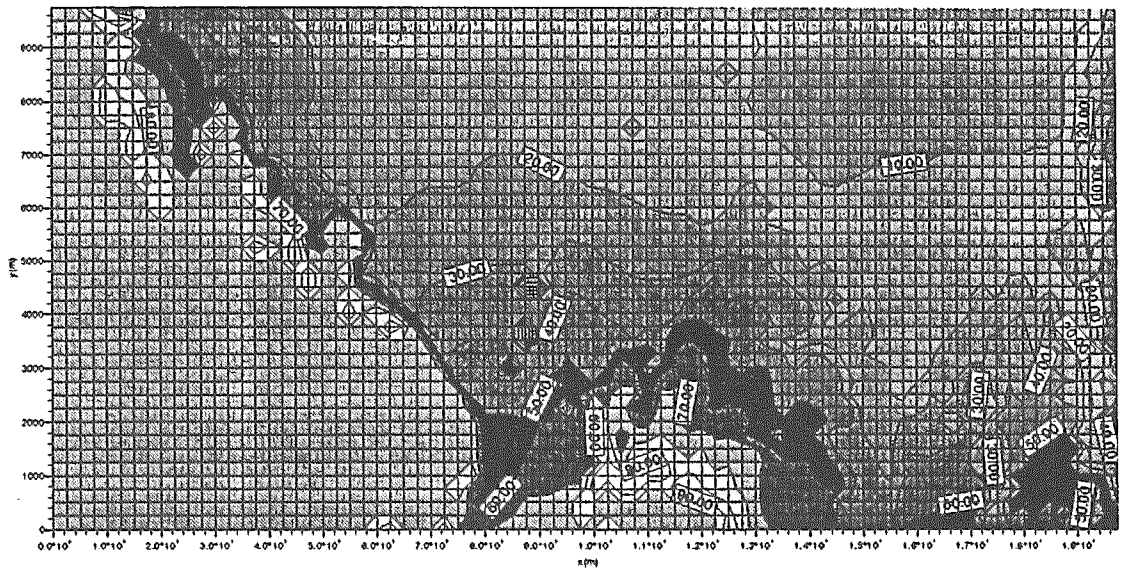

Figure-8 Eastern part of Sapporo

However, there are problems with using this national digital information (KS-124-1) for the calculation of flood flows: (1) the topographic data is supplied at a 250m grid, (2) river-related topographic data, such as embankments are excluded, and (3) the smallest unit is the meter. The problem with (1) is that flood flow calculations become limited by the 250m grid. In (2), even if information on river-related topography is added, the width of river and embankments is not realistic with the 250m grid. This is also the case for road widths.

Therefore, we replaced the 250m grid data with 50m grid data. However, the accuracy of the data remains the same and the minimum unit is still meters, which means that issue (3) remains unresolved. In our numerical calculations of flood flows, we cakulated the mean discharge in the direction of depth. Because the flood flow was considered to be shallow there is little change in depth in the direction of the discharge. A minimum 1m difference between topographic data in the calculation grid is not adequate. For the appropriate numerical simulation of flood flow, topographical data is the important key and improvements are urgently required.

CONCLUSION

The behavior of flood flows without initial depth is unpredictable and adequate simulation is

difficult. For example, when pouring water onto the ground, water flows from high to low, but it is difficult to predict accurately how the flowing water spreads.

In this study, we conducted a numerical simulation of flood flows in an urban area. To establish an appropriate model for predicting flood flows, a summary of the principal results and the remaining problems are: (1) the differential calculus of the basic equation are shown; (2) the numerical simulation of flood flows in an urban area could be conducted by assuming it to flow along street networks; (3) there is a lack of topographical data as well as data on the density of structures, etc. to be able to conduct flood flow calculations; (4) a more detailed data determination, possibly by remote sensing, is necessary for the future; (5) it is necessary to conduct model tests of future numerical simulations with more accurate data; and (6) there is a need to develop a number of appropriate flood flow models by considering boundary conditions, mainly as regards the lip of flood flows.

REFERENCES

1) Yasuyuki SHIMIZU: Flows of alluvial rivers and estimation methods of river bed deformation. Hokkaido University Paper for Doctor's Degree February, 1991 pp.48-73

2) Shoji FUKUOKA and Nobuo MATSUNAGA: Analysis of flood flows in an urban area with high density of structures and flood flow control. Civil Engineering Association, Hydraulics Committee, Water Engineering Paper, Vol.36 February, 1992 pp.311-316

3) Ministry of Construction, Geographical Survey Institute andNational Land Agency, Planning and Coordination Bureau: The national numerical information 1987 pp.1-130